Chapter 2

Cavity QED and the Road to Strong Coupling

2.1 "I Am Quantum. Hear Me Roar."

Crucial to the realization of manifestly quantum effects in cavity QED is *strong coupling*, a condition in which the coherent coupling between atom and cavity field dominates dissipative rates in the system. For a two-level atom optimally coupled to a cavity mode (see Figure 1.1), the dipole-field coupling is given by the Jaynes-Cummings interaction Hamiltonian [28]

$$\hat{H}_{int} = \hbar g_0(\hat{\sigma}^\dagger \hat{a} + \hat{\sigma}\hat{a}^\dagger), \tag{2.1}$$

where $(\hat{\sigma}^\dagger, \hat{\sigma})$ are dipole raising and lowering operators, $(\hat{a}, \hat{a}^\dagger)$ are field annihilation and creation operators for the cavity mode, and g_0 is one half of the single-photon Rabi frequency. This rate describes the exchange of excitation between the atomic dipole $\vec{\mu}$, initially in the ground state, and the electric field $\vec{E}_{1,cav}$ built up by a single photon of frequency ω residing in the mode volume V_m of the optical cavity:

$$\hbar g_0 = \vec{\mu} \cdot \vec{E}_{1,cav} = \mu \sqrt{\frac{\hbar\omega}{2\epsilon_0 V_m}}. \tag{2.2}$$

Thus g_0 is a rate of coherent evolution which must be compared with the dissipative rates for the system. These, in turn, are the atomic spontaneous emission rate $\gamma_\perp$

and the cavity field decay rate κ. While the regime of $(\kappa, \gamma_\perp) >> g_0$ is described by classical treatments, we will see that a quantum theory is necessary to account for physics at $g_0 >> (\kappa, \gamma_\perp)$, in the strong-coupling regime [29, 30, 31].

In a classical description of spectroscopy in an optical cavity, an atomic sample acts as a dispersive medium for the coherent light field circulating in the cavity mode volume. Classical behavior gives way to quantum as single quanta, whether of the atomic sample or of the light field itself, begin to induce nonlinear response in the system. To see how this may be accomplished, we begin with the familiar case of a "bulk" sample and consider how a strong interaction can be preserved as the number of particles is scaled down towards unity. This intuitive discussion is complemented by a more quantitative development in the following sections.

Consider first the interaction of light with a "bulk" atomic sample placed inside the cavity mode. The atoms in the sample scatter the optical field, producing a wavelength-dependent refractive index in the cavity mode volume. The atomic sample affects the resonance properties of the optical cavity if the atom-field interaction strength and the number of atoms are sufficient to noticeably alter the free-space dispersion relation for the light. Thus, if a single atom placed within the mode volume is to act as a nonlinear medium, it must have a large effective cross section for scattering intracavity light. First, then, the atom should have a near-resonant dipole interaction with the optical field mode supported by the cavity. Second, scattering should be enhanced by ensuring that optical wavefronts have every opportunity to interact with the atom in the process of being transmitted through the cavity. This second requirement is accomplished by constructing cavities with high finesse and tightly confined modes, so that light traverses the distance between the mirrors many times before exiting the cavity and furthermore has a high chance of interacting with the atomic cross section on each pass. Tight mode confinement has the additional benefit that the light is thoroughly diffractively mixed and thus the interaction is truly with a single cavity mode that is well defined throughout the interaction process. Quantitatively, the importance of a single atom for the response of the intracavity field is described by the single-atom cooperativity parameter $C_1 = g_0^2/2\gamma_\perp\kappa$, or by its inverse, the critical atom number, $N_0 = 2\gamma_\perp\kappa/g_0^2$ [31]. The single-atom cooperativity can be re-expressed in terms of familiar properties of the cavity (mode waist w_0 and finesse F) and the atomic transition (wavelength λ). One finds it scales simply as $C_1 \sim \frac{2F}{\pi}\frac{\lambda^2}{w_0^2}$, reflecting the requirements outlined above. Note that C_1 does not scale explicitly with the length of a Fabry-Perot cavity.

On the other side of the coin, consider the circumstances necessary to make the quantized nature of the light field relevant to observations of the cavity system. In the classical regime the cavity mode volume is occupied by a large-amplitude coherent field. To fully probe the atomic response function, the electric field associated with the light must be strong enough to saturate the atomic dipole. How, then, is a single photon to accomplish this saturation? Simply put, the photon must be confined to a small volume so its electric field strength within that volume becomes large. Indeed, making use of the single-photon Rabi frequency g_0, we can define a saturation photon number $m_0 = \gamma_\perp^2/2g_0^2$ [31]. As promised, this quantity is inversely proportional to the cavity mode volume through the factor $1/g_0^2$; it is, however, completely independent of the cavity finesse.

The physical significance of these critical parameters will be revisited in later sections. For now, we simply observe that if single quanta are to leave their stamp on observations in an optical cavity, the critical atom number and/or saturation photon number must satisfy $(N_0, m_0) \lesssim 1$. Note that these requirements imply $g_0 > \gamma_\perp$ but not necessarily $g_0 > \kappa$ as well. Thus manifestly quantum effects in cavity QED span a range of parameter regimes of which true strong coupling is only the most extreme. The transition from weak to strong coupling carries us from a classical description of light fields and scatterers to a regime in which the atom and cavity field must be considered as a single entity bound by a shared quantum of excitation.

2.2 Quantitative Description of the Atom-Cavity System

As is often the case, the conceptually and computationally simplest starting point for describing the atom-cavity system is the purely quantum limit, where the atom and cavity evolve via their coherent coupling in the absence of dissipation. This system simply obeys the Schrōdinger equation with the Jaynes-Cummings Hamiltonian [28],

$$H_{JC} = \hbar\omega \hat{a}^\dagger \hat{a} + \hbar\omega \hat{\sigma}^\dagger \hat{\sigma} + \hbar g_0 (\hat{a}\hat{\sigma}^\dagger + \hat{a}^\dagger \hat{\sigma}). \tag{2.3}$$

Here we consider a two-level atom and ω is the common resonance frequency of both atom and cavity. Diagonalizing this Hamiltonian gives rise to the well-known Jaynes-Cummings ladder of eigenstates for the coupled atom-cavity system, as illustrated in Figure 2.1. The coupled eigenstates are characterized by the equal sharing of excitation between the atomic dipole and cavity field, so that the n-excitation bare states $|g, n\rangle$ and $|e, n-1\rangle$ of energy $n\hbar\omega$ are replaced by

$$|\pm_n\rangle = \frac{1}{\sqrt{2}}(|g, n\rangle \pm |e, n-1\rangle) \tag{2.4}$$

with corresponding energy eigenvalues

$$E_{\pm_n} = n\hbar\omega \pm \sqrt{n}\hbar g_0. \tag{2.5}$$

To quantitatively predict actual atom-cavity dynamics, a treatment that moves beyond this idealized picture to include dissipation and driving terms will be necessary. Two qualitative features, however, are worth noting immediately from the Jaynes-Cummings ladder itself.

First, in the most fully quantum regime, the atom and cavity field are best described in a symmetric treatment where they combine to create a single entity sharing excitation equally. Most notably, for $n \geq 1$ excitation, there exist strong-field-seeking states $|-_n\rangle$ that can be thought of as atom-cavity states bound together by the shar-

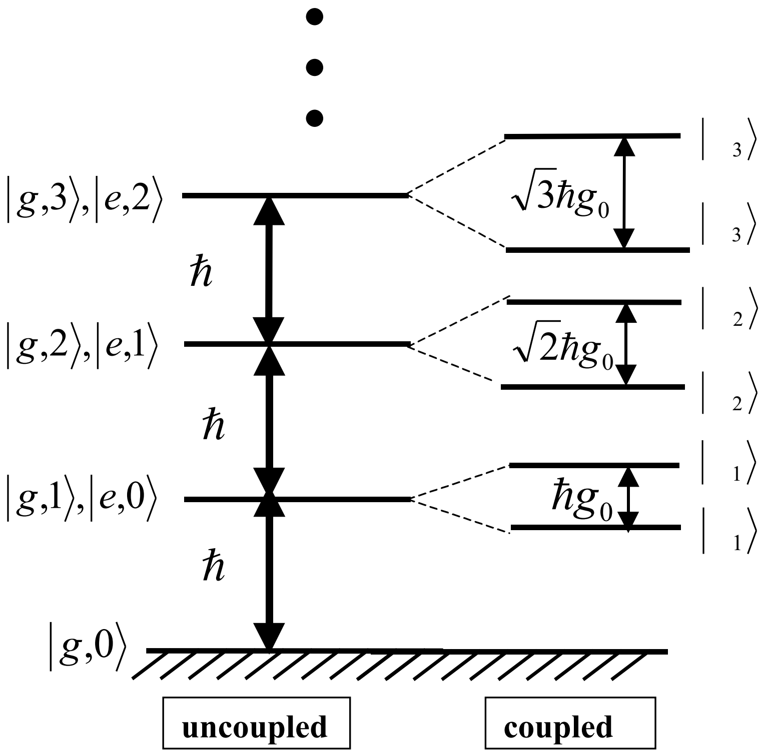

Figure 2.1: Jaynes-Cummings ladder of atom-cavity eigenstates

ing of a quantum of excitation. If we permit a detuning Δ_{ca} between the cavity and atom resonance frequencies, the sharing of excitation in these "bound states" becomes asymmetric but the qualitative properties of the ladder remain unchanged.

Second, while a ladder of strong-field- and weak-field-seeking states recalls the dressed states of atomic interaction with a coherent light field (e.g., in free space) [32], the Jaynes-Cummings ladder reflects atomic coupling to a small number of quantized excitations in the cavity mode rather than to a strong classical field in free space. The dressed state splitting at each level of the ladder is proportional to $\sqrt{n}$. In the limit of large n, many photons in the field, the ratio of splittings in successive levels is $\frac{\sqrt{n+1}}{\sqrt{n}} \rightarrow 1$; in this way we recover the free-space, classical-field ladder in which dressed states at each rung are split by a constant $\pm\hbar\Omega$.

In the cavity, on the other hand, where just a few excitations create a large response, the anharmonic nature of the level splittings with increasing n is a feature arising explicitly from the quantized nature of the cavity field. Thus, to observe effects of field quantization on the spectrum of atom-cavity response, we can expect that experiments must probe the saturation behavior of the system and not simply rely on spectroscopy in the weak-driving limit of $n < 1$ system excitations. One caveat to this observation, however, is that nonclassical aspects of the system *dynamics* can in fact be observed for weak driving; for example, photon statistics of the cavity output field in time are of interest even for experiments in the weak-excitation limit.

2.2.1 Master Equation in the Presence of Dissipation

In the presence of dissipation and driving, and allowing for detuning between the probe field and the atom and cavity resonant frequencies, the Jaynes-Cummings Hamiltonian becomes part of a master equation (see, e.g., [32, 33, 34]) for the joint atom-cavity density operator ρ. We consider a driving (and probing) field ϵ of frequency ω_p, a cavity resonant at $\omega_c = \omega_p + \Delta_{cp}$, and an atomic resonance frequency $\omega_a = \omega_p + \Delta_{ap}$. In the electric dipole and rotating-wave approximations, and in the interaction picture with respect to the probe frequency, the evolution is described by

$$\dot{\rho} = -\frac{i}{\hbar}[\hat{H}_0, \rho] + \gamma_\perp(2\hat{\sigma}\rho\hat{\sigma}^\dagger - \hat{\sigma}^\dagger\hat{\sigma}\rho - \rho\hat{\sigma}^\dagger\hat{\sigma}) + \kappa(2\hat{a}\rho\hat{a}^\dagger - \hat{a}^\dagger\hat{a}\rho - \rho\hat{a}^\dagger\hat{a}), \qquad (2.6)$$

$$\hat{H}_0 = \hbar\Delta_{cp}\hat{a}^\dagger\hat{a} + \hbar\Delta_{ap}\hat{\sigma}^\dagger\hat{\sigma} + \hbar g(\vec{r})[\hat{a}\hat{\sigma}^\dagger + \hat{a}^\dagger\hat{\sigma}] + \hbar\epsilon(\hat{a} + \hat{a}^\dagger). \qquad (2.7)$$

Here $g(\vec{r})$ is the coupling strength which takes into account the atomic position $\vec{r}$ within the cavity mode. For a Fabry-Perot cavity supporting a standing wave mode with Gaussian transverse profile, $g(\vec{r}) = g_0\psi(\vec{r}) = g_0 cos(2\pi x/\lambda)exp[-(y^2 + z^2)/w_0^2]$. The cylindrical symmetry of $\psi(\vec{r})$ suggests the use of cylindrical coordinates (ρ, θ, x), in which case we write $g(\vec{r}) = g_0 cos(2\pi x/\lambda)exp[-\rho^2/w_0^2]$. In the fully quantum treatment, the atomic position $\vec{r}$ is itself an operator; in experiments to date a quasi-classical treatment suffices, so the atom may be considered a wavepacket with $\vec{r}$ a classical center-of-mass position variable.

This master equation provides a valid description of the atom-cavity system in any range of parameters $(g_0, \kappa, \gamma_\perp)$. It can in general be solved only numerically, but certain limits, either of inherent rates or of driving strengths, permit analytical treatments of limited application. In the sections below, we discuss behavior exhibited by theory and experiment in several different parameter regimes from semiclassical to very strongly coupled.

2.3 Semiclassical Approximation: Optical Bistability

Certain parameter regimes are well described by an approximation in which we derive from Equations 2.6-2.7 the equations of motion for the expectation values of atom and cavity properties, i.e., $\langle \hat{a} \rangle$ and $\langle \hat{\sigma} \rangle$; then within these equations of motion all joint atom-cavity operator moments are assumed to factor, e.g., $\langle \hat{a}^\dagger \hat{\sigma} \rangle = \langle \hat{a}^\dagger \rangle \langle \hat{\sigma} \rangle$. This corresponds to a semiclassical treatment in which the field is described by its coherent amplitude $\langle \hat{a} \rangle = \alpha$. Such a replacement is valid in the limit of large critical parameters $(N_0, m_0) >> 1$, in which case a collection of atoms acts as a classical nonlinear intracavity medium. Within this approximation, Equations 2.6-2.7 yield an analytic expression for the driving field $\epsilon = \kappa\sqrt{m_0}Y$ as a function of the intracavity field $\langle \hat{a} \rangle \leftrightarrow \sqrt{m_0}X$. This relation is the well known optical bistability state equation [35]:

$$Y = X[(1 + \frac{2C}{1+\delta^2+X^2} + i(\phi - \frac{2C\delta}{1+\delta^2+X^2})]. \tag{2.8}$$

Here we have employed the standard notation for the bistability equation, related to our previous discussions by detunings $\delta = \Delta_{ap}/\gamma_\perp$ and $\phi = \Delta_{cp}/\kappa$, and N-atom cooperativity parameter $C = NC_1$.

The system saturation behavior described by this relation is shown in the dotted curve of Figure 2.2. The figure plots T, the ratio of full-cavity to empty-cavity transmission, as a function of input driving strength expressed in units of the steady-state photon number $\bar{n}_0$ in the empty cavity. The calculation shown is actually for a system in the strong-coupling regime, namely the cavity of Ref. [20], with $\omega_a = \omega_c$ and ω_p detuned 20 MHz below resonance. Here the bistability prediction is at variance with the quantum prediction and with actual system behavior, as discussed later in

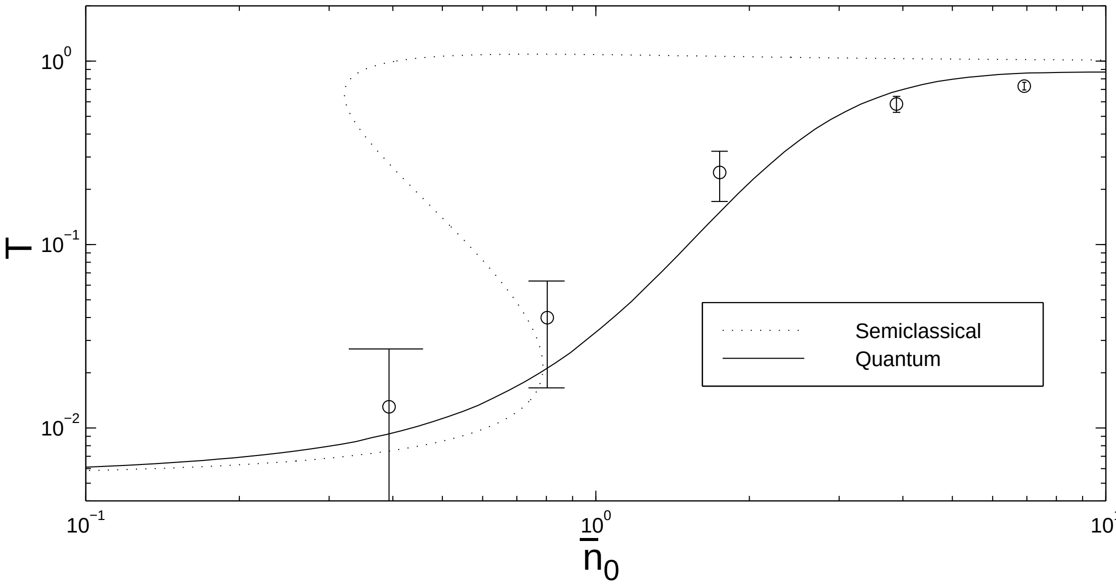

Figure 2.2: Semiclassical and quantum saturation predictions for parameters $(g_0, \kappa, \gamma_\perp)/2\pi = (120, 40, 2.6)$ MHz and $(\omega_a = \omega_c = \omega_p + 2\pi(20\,\mathrm{MHz}))$. T, the ratio of full-cavity to empty-cavity transmission, is plotted as a function of input driving strength $\overline{n}_0$ (in units of empty-cavity photon number). Experimental data is shown as circles with error bars.

this chapter. In the optical bistability state equation the correspondence between the semiclassical amplitude X and the actual operator expectation value $\langle \hat{a} \rangle$ is only approximate; in general the intracavity state is not an exact coherent state, but the bistability equation gives an input-output relation between the driving power $\sim Y^2$ and a transmitted photocurrent $\sim X^2$ which is valid insofar as the underlying approximation is justified.

Optical bistability effects in general have a long history in measurements within the context of laser physics. Specific cavity QED experiments measuring optical bistability in two-level systems date from the early 1980's [36, 37] and are realizable in relatively low-finesse cavities interacting with a sample of atoms crossing the cavity mode in a thermal atomic beam. However, the bistability state equation is also valid when $(N_0, m_0) < 1$ in the special case of very weak driving, $n << 1$ excitations in the system. In this case, only the first $(n = 1)$ excited states of the system must be considered, and the resulting relationship of joint operator moments makes factoring formally valid. The correspondence is reflected in the coincidence of the quantum and semiclassical curves of Figure 2.2 at very low driving strength. This fact comes as no surprise in the light of our earlier discussion of the Jaynes-Cummings ladder; the structure of the spectrum reflects the quantized field only for higher drive strengths that sample the anharmonicity of the system eigenvalues. Optical bistability also describes the steady-state behavior of an atom-cavity system where inherent strong coupling is washed out by the simultaneous interaction of many atoms with the cavity mode.

Even in the regime of the optical bistability equation, nonclassical dynamics of the atom-cavity system are accessible. Experiments measuring the photon statistics of the cavity output field have demonstrated nonclassical correlation functions of the output light, with similar work pushing from this limit to the inherently strong-coupling regime [38, 39, 40, 41].

2.4 Interacting Single Quanta: The 1-D Atom

By increasing cavity finesse and decreasing mode volume, we move to a regime of small critical parameters $(N_0, m_0) < 1$. Here single atoms and photons induce nonlinear effects in the system response. However, this condition is still consistent with overall dissipative dynamics if the cavity decay rate is fast relative to the coherent coupling g_0. This regime, known as the "bad cavity" limit, is realized for $\kappa > g_0^2/\kappa > \gamma_\perp$. In this limit, single quanta within the cavity mode interact strongly with one another, but coherence and information leak rapidly from the system into the output channel defined by cavity decay. Thus the atom-cavity coupling is essentially perturbative, and the atom and cavity each retain their distinct identities but with decay rates modified by the interaction. For instance, an atomic excitation, rather than decaying via spontaneous emission at rate $\gamma_\perp$, is much more likely to be exchanged into the cavity field and subsequently decay via the cavity; this preferential decay via the cavity mode at rate g_0^2/κ gives an effectively "1-D atom."

Experiments in this parameter regime include the quantum phase gate [42] and the use of squeezed light in cavity QED [43]. Both of these effects involve the production of nonclassical effects on the light field due to nonlinearities mediated by a "1-D atom" phenomenon. Thus single photons can interact with one another by means of their common coupling to an intracavity atom. These effects are seen with single strongly-coupled atoms; since these experiments delivered atoms to the cavity via thermal beams of atoms transiting a cavity mode, a background of weakly coupled or "spectator" atoms acted to dilute the inherent single-atom effect. Nevertheless, the essential character of the effects was accessible with strongly-coupled atoms flying across the cavity mode quickly against a background of spectators in the wings of the cavity mode.

2.5 Strong Coupling: Vacuum Rabi Splitting, Trapping, and Sensing

By further increasing cavity finesse, we arrive at the regime of strong coupling for the atom-cavity system. In this regime, where $g_0 >> (\kappa, \gamma_\perp)$, single quanta are significant and, furthermore, their coherent interaction dominates other rates in the system. It is in this limit that observations most closely reflect the ideal structure of the Jaynes-Cummings ladder. Exchange of excitation at rate g_0 is no longer perturbative, and the system crosses over to a set of joint atom-cavity eigenstates with widths set by decay rates κ and $\gamma_\perp$. The coupled atom-cavity transmission spectrum reflects this eigenvalue structure via the vacuum Rabi splitting [44], in which the empty-cavity Lorentzian line profile is transformed into a double-peaked transmission function as shown in Figure 2.3 and first directly observed in [45]. The positions and widths of the vacuum Rabi sidebands depend on the strength of the driving field ϵ as well as the parameters $(g(\vec{r}), \kappa, \gamma_\perp)$, and are found via steady-state numerical solution of the master equation.

To fully realize the quantum mechanical phenomena inherent in Equations 2.6-2.7 for strong coupling, yet another rate must be made small relative to the coherent cou-

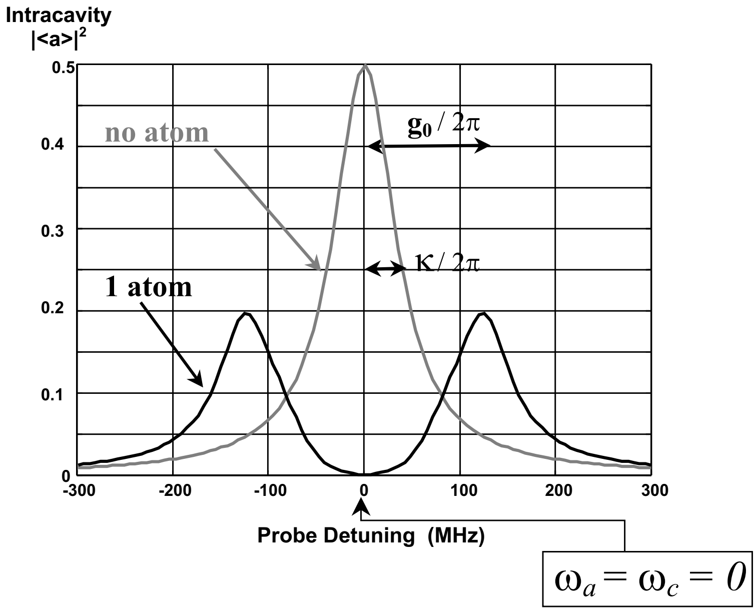

Figure 2.3: Vacuum Rabi splitting for $(g_0, \kappa, \gamma_\perp) = 2\pi(120, 40, 2.6)$ MHz and 0.5 photons in the empty cavity on resonance. Intracavity $|\langle a \rangle|^2$, from steady-state solution of the master equation, is plotted as a function of probe detuning $(\omega_p - \omega_a)/2\pi$.

pling. This is the rate for decoherence as information exits the system via movement of the individual atoms contributing to the effective atom number N. If excitation is distributed among an ensemble of atoms, each poorly coupled or coupled for a short time as it flies across the cavity mode, the true structure of the single-atom Jaynes-Cummings ladder cannot be observed. Thus experiments designed to probe the strong coupling regime must be carried out with cold atoms, in a situation where atom number $N \sim 1$ is realized through an actual single atom strongly coupled for a time τ satisfying $1/\tau << g_0$. Experiments of this type to date have involved a cloud of atoms trapped in a magneto-optical trap (MOT), cooled via standard sub-Doppler techniques, and then dropped or launched so that single atoms arrive in the cavity mode volume with small velocities and interact one at a time with the cavity field. Such an experiment is shown schematically in Figure 2.4; single atoms fall through the cavity mode and are detected via real-time changes in the transmission of a continuously monitored cavity probe beam [46, 20, 47, 48, 49]. More recently, single atoms have also been caught within the cavity by means of the quantized field [25, 50] or trapped there using a separate far-off-resonance trap (FORT) [51, 52]. Other efforts

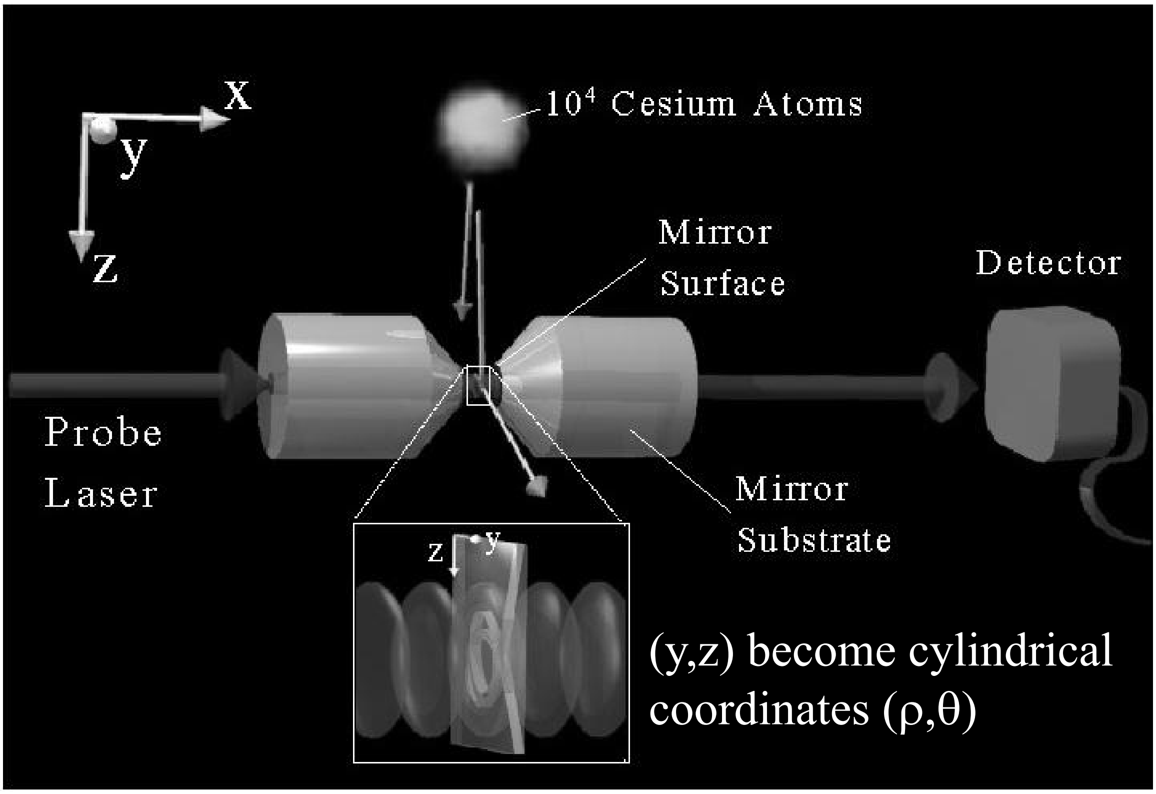

Figure 2.4: Schematic experiment with cold atoms in cavity QED.

in progress include the use of cavities with magnetic traps for atoms [53], trapped and cooled ions [54, 55], and FORTs chaining atoms through the cavity in the transverse direction [56, 57].

Cavity QED with cold atoms in the strong coupling regime has enabled observation of the vacuum Rabi splitting for single atoms in an optical cavity, and of the quantum saturation of the atom-cavity response. In Ref. [20], for example, measurements of cavity transmission vs. input driving field strength clearly deviate from the prediction of the optical bistability equation and are instead consistent with numerical solutions of the quantum master equation itself (Figure 2.2, solid line and experimental data points). This work was carried out with laser-cooled Cesium atoms dropped through an optical cavity of length $l = 10.1\ \mu m$ and finesse $F = 180,000$, leading to $(g_0, \kappa, \gamma_\perp) = 2\pi(120, 40, 2.6)$ MHz and critical parameters $(N_0, m_0) = (0.014, 2 \cdot 10^{-4})$. This and subsequent experiments [25, 50, 51] thus operate in a regime of critical atom number and saturation photon number orders of magnitude below unity. In this case driving fields which populate the cavity mode with coherent amplitudes at or even below one photon are sufficient to induce nonlinear response in the system. Likewise, effective atom numbers well below one interact strongly with the cavity field and alter the cavity transmission spectrum. Therefore the presence of a single atom, even when poorly coupled or just entering the cavity mode volume, can be detected with high signal-to-noise via the transmission of a probe beam through the cavity.

2.5.1 Real-Time Detection and Trapping with Single Photons

A striking demonstration of strong coupling in optical cavity QED comes in recent experiments which actually bind an atom in the cavity by creating the "bound-state" $|-\rangle$ of the Jaynes-Cummings ladder [25, 50]. Figure 2.5(a) shows the ladder of atom-cavity energy eigenvalues with emphasis on the continuous evolution from bare to joint eigenstates as a function of atom-cavity coupling, and therefore of atomic position within the cavity mode. As an atom falls through the Gaussian transverse profile of the cavity mode, the eigenvalues evolve as illustrated in the figure. Concentrating on the ground and first excited states of the manifold, we will see that this eigenvalue structure enables both sensing and trapping of an atom by means of the cavity field.

If the cavity is probed at its bare resonance frequency $\omega_p \approx \omega_c$, we see from Figure 2.5 that this probe will be moved out of resonance as the atom-cavity coupling increases, causing a drop in transmitted light as an atom moves into the cavity. If, on the other hand, the probe is tuned below the cavity resonance $\omega_p < \omega_c$ and instead near the lower dressed state, it will move into resonance as an atom becomes more strongly coupled. In this case the cavity transmission is originally low and increases as an atom moves toward regions of strong coupling. To see these effects quantitatively, we find steady-state solutions of the master equation to obtain the vacuum Rabi spectrum in Figure 2.5(b). This spectrum has been calculated for the experimental parameters of Ref. [25]. As seen already in the data of Ref. [20], resonant probe transmission can be reduced by factors of $10^2 - 10^3$, providing enormous signal-to-

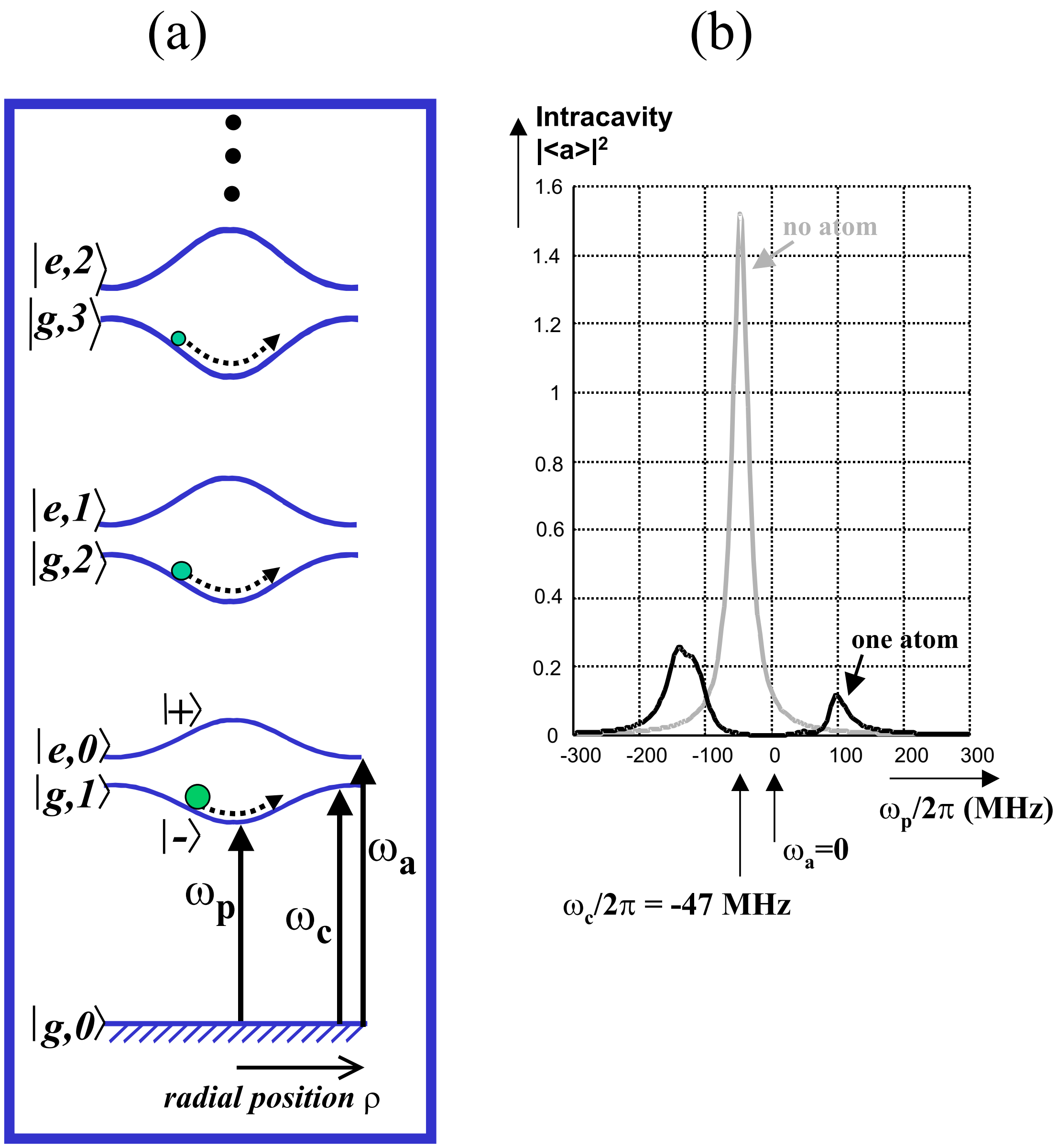

Figure 2.5: (a) Atomic-position-dependent eigenstates and (b) calculated vacuum Rabi splitting for triggered trapping experiments. Here $(g_0, \kappa, \gamma_\perp)/2\pi = (110, 14.2, 2.6)$ MHz, $(\omega_c - \omega_a)/2\pi = -47$ MHz, and the drive strength corresponds to 1.56 photons in the empty cavity on resonance.

noise for detection of an intracavity atom. For a probe on the lower vacuum Rabi sideband, the transmission increase is less drastic, but probing at this frequency is nevertheless often preferable because of its effect on the atomic motion.

Thus far we have discussed strong coupling between the cavity field and atomic dipole, or internal state. We can define a further condition of strong coupling for the *external* atomic degrees of freedom, which occurs when the coherent coupling dominates the atomic kinetic energy as well. Under these circumstances the position-dependent energy eigenvalues cause an important mechanical effect on an atom interacting with the cavity mode. For instance, an attractive effective potential is felt by an atom when a probe field tuned to the lower vacuum Rabi sideband is used to populate the strong-field-seeking state $|-\rangle$. When this potential is large relative to the atomic kinetic energy, experimental observations range from atom-cavity scattering effects to largely conservative binding of an atom by a single-photon cavity field [20, 50, 25, 26]. The ability to both trap an atom and sense its motion in real time leads naturally to schemes to actively cool an atom in the cavity.

2.6 Broader Application of Real-Time Sensing Capabilities

Optical cavity QED in the strong coupling regime provides, as we have seen, a nearly closed environment for interactions between single quanta. Furthermore, it retains the chief merit of optical cavity spectroscopy in the classical regime: enhanced signal-to-noise for observation of intracavity dynamics through the well-defined output channel of cavity decay. While in the language of open quantum systems the cavity decay at rate κ introduces decoherence into the system, the decay is a single output mode which can be directed toward some use which actually keeps information within the broader system of interest. In the context of optimal state estimation and control, this may mean measuring the transmitted field and using that information to control the system via active feedback. In the case of quantum logic and communication, it may mean measuring the output field or sending it efficiently to a distant cavity to be coherently interacted with a second atom there.

One measure of the capability for observation is the so-called *optical information* rate for monitoring intracavity dynamics through measurement of transmitted light. For a simple estimate of optical information, we consider the case of a resonant probe, $\omega_p = \omega_c = \omega_a$, whose transmission drops as an atom enters the cavity mode. The presence of an atom is thus signaled by a rate dI/dt of "missing" photons at the cavity output. This rate is given by $dI/dt = \kappa(|\langle a\rangle|^2_{empty} - |\langle a\rangle|^2_{full}) \approx \kappa|\langle a\rangle|^2_{empty}$ provided that $|\langle a\rangle|^2_{full}$ is very small. This is the case for strong coupling conditions but driving strength still small enough to prevent complete saturation of the atomic response. Thus dI/dt is maximized for $|\langle a\rangle|^2_{full} \approx m_0$ and $|\langle a\rangle|^2_{empty} \approx C_1^2|\langle a\rangle|^2_{full} \approx g_0^2/\kappa^2$. This rough argument yields an optical information rate $dI/dt = g_0^2/\kappa$; the same quantity appears in a formal treatment of the resonant-probing case as well as in calculations of probing on the lower vacuum Rabi sideband and in analytic expressions for various schemes to monitor both atomic position and atom-cavity internal states in a strong-driving limit [58].

2.6.1 More Intuitive Arguments for Optical Information and Critical Parameters

What can we say about the physical significance of g_0^2/κ? A key question seems to be: How much does the atom prefer coupling into the cavity over coupling into the ordinary vacuum modes available? The quantity g_0 can be simply understood via

$$\frac{g_0^2}{\gamma_\perp^2} \propto \frac{\textit{atomic radiative volume}}{\textit{cavity mode volume}}. \tag{2.9}$$

How does this relate to our previous definition (from Section 2.1) of $\hbar g_0 = \vec{\mu}\cdot\vec{E}_{1,cav}$ where $\vec{E}_{1,cav}$ is the electric field of a single photon in the cavity mode? The atomic decay rate $\gamma_\perp$ is itself given by $\vec{\mu}\cdot\vec{E}_{1,rad}$ where $\vec{E}_{1,rad}$ is the electric field of a single photon in the atomic radiative volume; this relationship can be viewed as defining the atomic radiative volume. Alternatively the atomic radiative volume can be roughly set as $\sim \lambda^2 \cdot (c/\gamma_\perp)$, i.e., a cross-sectional area $\sim \lambda^2$ extending over a distance $c/\gamma_\perp$. If we remember $\gamma_\perp \propto \mu^2/\lambda^3$ from the Fermi golden rule, and employ $E_{1,rad} \propto \sqrt{\hbar\omega/V_{rad}}$, a few lines of algebra will show the internal consistency of these relations. Either way, we then recall that the electric field of a single photon confined to a given mode volume is inversely proportional to the square root of that mode volume, yielding the relationship stated above in Equation 2.9.

Since it takes half a photon per radiative volume to saturate the atom, it takes $\gamma_\perp^2/2g_0^2$ photons per cavity volume for saturation, neatly providing the saturation photon number m_0.

Now consider some (saturating) excitation shared between atom and field. The atomic spontaneous emission can dump excitation at rate $\gamma_\perp$, while the cavity sheds whatever it has at rate 2κ. But the cavity only needs to hold m_0 of excitation to saturate the atom, so the cavity is dumping excitation at overall rate $m_0(2\kappa) = \frac{\gamma_\perp^2}{2g_0^2}(2\kappa)$. Thus the rate of overall system decay through the atom compares to that through the cavity as

$$\frac{\Gamma_{sys,atom}}{\Gamma_{sys,cavity}} = \frac{\gamma_\perp}{\frac{\gamma_\perp^2}{2g_0^2}2\kappa} = \frac{g_0^2}{\kappa\gamma_\perp} = 2C_1 = 2/N_0. \tag{2.10}$$

The critical atom number then shows up as roughly the number of atoms necessary to partner equally with the cavity in disposal of shared excitation.

Finally, suppose we are driving the cavity (on resonance) with enough power to keep the system saturated at roughly one excitation in the atom and m_0 excitations in the cavity mode. The system is acting like one part empty cavity to $2C_1$ parts excitation-eating, atom-related beast. If we take the atom away, two things will happen. First, a factor of $2C_1$ more driving light will actually get into the system to produce excitation, since before only the empty-cavity-like part was resonant with the drive and now the whole system is. Second, all the excitation that does get in will decay through the cavity since no other channel remains. That means another factor of $2C_1$. Actually these are factors of $(1 + 2C_1)/1$, but if we assume the cooperativity is large we need not worry about the difference. So the additional cavity output signal that tells us the atom is gone is given by the original output rate, $m_0\kappa = \frac{\gamma_\perp^2}{2g_0^2}\kappa$, multiplied by $(2C_1)^2 = \frac{g_0^4}{\kappa^2\gamma_\perp^2}$. This gives us (again to within the ever-present factor of two) the magical quantity g_0^2/κ, and we have stuck to our original resolution not to lift a pencil.

While by no means airtight, these lines of argument at least give some sense of the optical information as meaning something basic about the atom-cavity interaction.

2.6.2 What is the Information Good For?

The quantity $dI/dt = g_0^2/\kappa$ corresponds to information about some aspect of the atom-cavity state accessible at a rate of over 10^9 per second for the current generation of strong-coupling Fabry-Perot cavities with alkali atoms. This must be compared with a rate for monitoring the same atom via light scattering in free space, where fluorescence rates do not exceed $\approx 10^7$ per second and it is nearly impossible to imagine efficient collection of the light emitted over 4π solid angle. This orders-of-magnitude increase in detection capability represents one of the main strengths of cavity QED in quantum state control.

This sensing ability can be brought to bear in diverse ways. In a current experiment [51, 52], an atom entering the cavity mode is detected via cavity QED and then trapped by a separate light field in a different longitudinal mode of the cavity. This far-off-resonant trap (FORT) takes advantage of the cavity buildup power to obtain intensities large enough to trap the atom even in the face of mechanical effects caused by the cavity QED probe field. The sensing ability provided by that probe field allows trapping of one and only one atom in the FORT, opening the door for schemes in quantum information science that rely on deterministic interaction of a single atom with the field.

Many such schemes fall under the general heading of quantum state synthesis, using the single-atom medium to prepare single photons and other nonclassical states of the light field. Existing methods of single-photon generation encounter difficulty in providing true determinism of the output field, either in timing or in spatial output channel. The output channel difficulty is naturally solved in cavity QED, and efficient single-atom trapping is bringing true on-demand state generation within the realm of possibility. Proposals encompass not only single-photon generation but also numerous other state preparations, such as the photon turnstile and the single-atom laser (see, e.g., [59]), as well as schemes for entanglement generation made possible by the high detection efficiencies [60].

Another direction which relies on real-time sensing in cavity QED is quantum state estimation and quantum feedback. Real-time active feedback methods infer the system state and steer it toward some target value; as cavity-assisted state measurement approaches its fundamental quantum limit, a servo will be limited by measurement backaction effects. Performance of such a control loop will depend on minimal-disturbance measurements for the variable of interest, and the dynamics should exhibit the evolution-and-collapse patterns characteristic of quantum trajectory theory [61, 62]. Experiments on real-time feedback to atomic position explore this issue from one direction, but the concept applies equally to other aspects of the overall atom-cavity state. For instance, ongoing experiments [63] also apply real-time sensing and feedback towards the goal of designing novel states of the cavity output field itself.